International Journal of Nanomedicine

Dovepress
Taylor & Francis Group

Open Access Full Text Article

ORIGINAL RESEARCH

Liposomal Co-Delivery of Antigenic Glycan LDNF and α-GalCer Elicits Potent IgG Responses with Potential for Anti-Helminth Immunity

Qianghui Tang[1,*], Qiang Chao[2,*], Jianfeng Zhang[2], Bei Wang[2], Song Zhao[2], Kun Yang[1,2]

[1]Wuxi School of Medicine, Jiangnan University, Wuxi, Jiangsu, People's Republic of China; [2]Key Laboratory of National Health Commission on Parasitic Disease Control and Prevention, Jiangsu Institute of Parasitic Diseases, Wuxi, People's Republic of China

*These authors contributed equally to this work

Correspondence: Kun Yang, Wuxi School of Medicine, Jiangnan University, Wuxi, Jiangsu, People's Republic of China, Email yangkun@jipd.com; Song Zhao, Key Laboratory of National Health Commission on Parasitic Disease Control and Prevention, Jiangsu Institute of Parasitic Diseases, Wuxi, Jiangsu, People's Republic of China, Email shanechn@163.com

Introduction: Parasitic worms (helminths) express unique antigenic glycans such as LDN and LDNF, which are absent in mammalian hosts and represent promising vaccine targets. However, free glycans typically elicit weak immune responses and require multivalent delivery and adjuvants to enhance immunogenicity and promote antibody class-switching.

Methods: Two cetyl-modified glycan antigens (LDN-C16 and LDNF-C16) were chemo-enzymatically synthesized and incorporated into liposomes, either with or without the invariant natural killer T cell agonist α-GalCer as an adjuvant. C57BL/6 mice were immunized subcutaneously. Humoral immune responses were evaluated by ELISA using glycan-BSA conjugates. Cytokine levels were measured in sera from immunized mice. Additionally, the ability of immune sera to recognize native helminth proteins was assessed by Western blotting using protein extracts from adult *Schistosoma japonicum* worms.

Results: Liposomal delivery of LDNF, but not LDN, induced potent glycan-specific antibody responses. Adding α-GalCer slightly reduced total antibody titers but enhanced response quality by shifting IgM to IgG, increasing IgG1 and decreasing IgG2b. Liposomal LDNF with α-GalCer also boosted in vivo cytokine responses, increasing IL-4 and IL-10 while maintaining IFN-γ. The induced antibodies showed high specificity for LDNF and effective recognition of native schistosome worm proteins.

Conclusion: Liposomal presentation of the LDNF epitope strongly enhances immunogenicity. Co-delivery with α-GalCer effectively promotes class-switched IgG responses, modulates cytokine profiles, and improves recognition of native parasite antigens. This liposomal glycan-antigen delivery strategy represents a promising approach for the development of anti-helminth vaccines targeting glycan epitopes.

Keywords: helminth glycans, vaccine target, liposome nanoparticles, α-galcer adjuvant, antibody class switching

Introduction

Parasitic worm (helminth) infections represent a long-neglected category of parasitic disease. Flukes, tapeworms, and nematodes invade their hosts via contaminated water, food, or soil, thereby establishing chronic infections in the intestines, bloodstream, or internal organs. These infections result in diverse pathologies including malnutrition, growth retardation, and hepatic fibrosis, thereby imposing a substantial burden on global public health.[1–5] Currently, there are no effective advanced solutions for the diagnosis, treatment, or prevention of helminth infections.

The complex carbohydrates expressed by helminths offer a promising avenue to address these diagnostic and therapeutic gaps. Helminth glycan profiles are markedly distinct from those of mammalian hosts. For instance, many helminths lack GalNAcβ1-4GlcNAc-R (LN) and terminal sialylation modifications; instead, they display terminal structures, such as GalNAcβ1-4GlcNAc-R (LDN) and its fucosylated derivative GalNAcβ1-4(Fucα1-3)GlcNAc-R (LDNF), as observed in *Trichinella spiralis, Fasciola hepatica, Dictyocaulus viviparus* and various schistosome species.

https://doi.org/10.2147/IJN.S590048
Received: 19 December 2025
Accepted: 17 March 2026
Published: 8 April 2026

Graphical Abstract

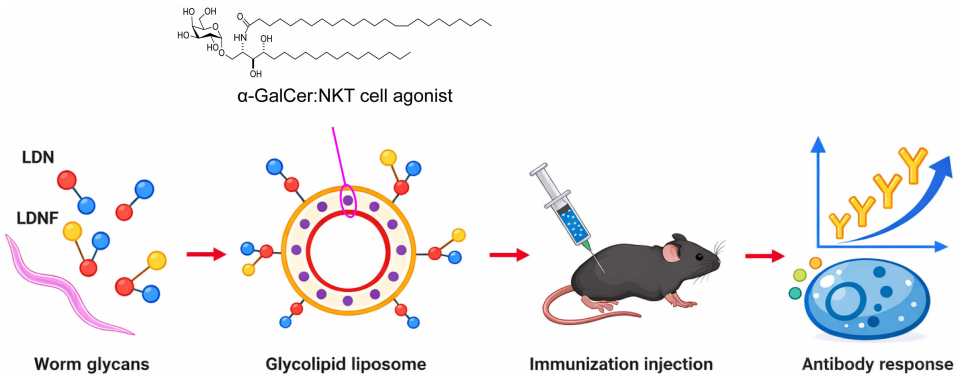

Moreover, unique core modifications such as α1,3-fucose and β1,2-xylose are present in certain helminths (Figure 1A).[6,7] These glycans, which are absent in humans, are abundantly expressed on the parasite surface and in excretory/secretory products. They serve as key foreign antigens recognized by the immune system, and are closely associated with helminth pathogenicity and immunomodulatory functions.[8–10]

During helminth infections, antigen-presenting cells such as dendritic cells recognize these glycans via pattern recognition receptors (eg., C-type lectin receptors). Following processing and presentation, they drive naïve T cells to differentiate into specific T helper subsets (eg., Th1, Th2, Treg) and promote the secretion of specific cytokines. These cytokines then mediate effector functions, including B cell activation and specific antibody production (Figure 1B).[8,11,12] Epidemiological evidence supports this mechanism: in *Schistosoma mansoni* (*S. mansoni*)-endemic regions, serological studies comparing newly arrived immigrants and long-term residents demonstrated common detection of antibodies against LDN and LDNF (including the LDN-DF variant), with response profiles varying by age and exposure duration.[13] Serum samples from individuals infected with multiple filarial parasites, analyzed using a Brugia malayi-derived glycan array, revealed widespread anti-glycan IgG responses with distinct patterns across different infection states, suggesting that such responses may serve as biomarkers of exposure or infection.[14] Furthermore, in rhesus monkey and mouse infection models, sera from *S. mansoni*-infected animals rich in anti-glycan antibodies can kill schistosomes in vitro through antibody-dependent cellular cytotoxicity (ADCC) and complement activation.[15] Monoclonal IgM antibodies targeting the LDN epitope have been found to induce the lysis of schistosome larvae in vitro through a complement-dependent mechanism.[16] In a vaccine study against the nematode *Haemonchus contortus* in lambs, a formulation containing nematode excretory/secretory (ES) glycoproteins plus an adjuvant conferred effective protection, with strong IgG responses correlating with antibodies against antigenic glycans, particularly LDNF.[17]

Therefore, the development of vaccines that target helminth glycan epitopes is an attractive strategy. However, oligosaccharides alone elicit relatively weak antibody responses, often inducing IgM production without robust class switching.[18,19] To further induce high-affinity antibodies and durable immune memory, it is necessary to present glycan epitopes in a multivalent form and effectively drive B cells to undergo class switching from IgM to IgG.[20,21] Nanoparticles (such as liposomes) represent an attractive delivery platform because they can display multiple copies of glycolipid antigens in a membrane-like environment, enhancing B cell recognition and activation.[22] Furthermore, incorporating immunomodulatory lipids can engage specific lymphocyte subsets to provide "help." Presentation of glycolipid antigens by CD1 molecules is a well-established immunological mechanism. In particular, CD1d-restricted presentation of synthetic glycolipids, such as α-GalCer, is known to potently activate iNKT cells.[23–26] Activated iNKT cells rapidly secrete cytokines that can provide T-helper-like signals to B cells, promoting antibody class switching (particularly IgG) and affinity maturation.[27,28] Thus, co-delivery of glycan antigens and α-GalCer within liposomes may synergistically enhance the quality and magnitude of anti-glycan antibody responses. To validate the in vivo efficacy of

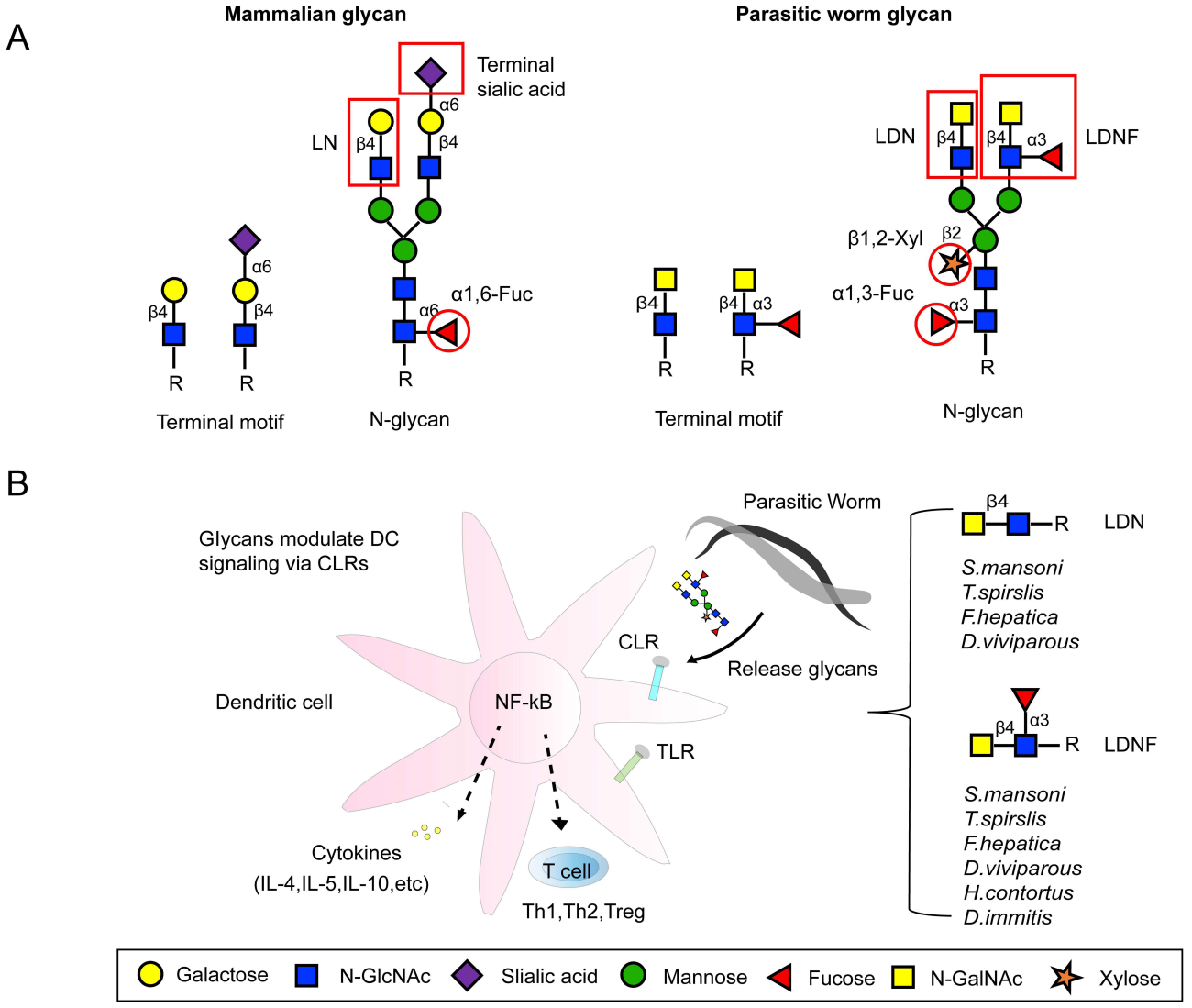

Figure 1 Glycan structural variations and their immunomodulatory roles. (**A**) Comparison of representative glycan structures expressed in mammals versus parasitic helminths. Red circles indicate N-glycan core modifications (α1,3/6-Fuc or β1,2-Xyl); Red boxes indicate representative terminal glycan motifs, including LN, terminal sialic acid, LDN, and LDNF. (**B**) Schematic of immune recognition: helminth-derived glycans are recognized by CLRs and TLRs on dendritic cells, thereby modulating subsequent immune responses.

this glycan delivery platform, selection of an appropriate animal model is of critical importance. C57BL/6 is the optimal mouse strain for this work. First, it is the most widely used model in both glycan immunology and preclinical development of liposomal vaccine systems.[29–31] Second, it is the best-characterized genetic background for investigating iNKT cell biology and α-GalCer-mediated activation.[24,31,32] Third, its genetic background supports a balanced Th1/Th2 immune profile, which is essential for comprehensive assessment of class-switched IgG subtype responses induced by our glycoconjugate vaccine.[33,34]

In this study, we chemo-enzymatically synthesized cetyl (C16)-modified glycan antigens—the disaccharide (LDN-C16) and the trisaccharide (LDNF-C16). These glycan antigens were then assembled with dioleoylphosphatidylcholine (DOPC) and cholesterol (CH) to form nanoliposomes with α-GalCer selectively incorporated as an immunostimulatory adjuvant. We systematically characterized the physicochemical properties of liposomes and evaluated their capacity to elicit glycan-specific antibodies in a C57BL/6 mouse model. These results demonstrated that liposomal delivery markedly enhanced the immunogenicity of LDNF, whereas co-encapsulation with α-GalCer further promoted antibody class switching toward IgG subclasses, thereby refining the quality of the humoral immune response. Consistent with

https://doi.org/10.2147/IJN.S590048

previous studies on carbohydrate/lipid-based antigen mechanisms, this study demonstrates that liposomal delivery of synthetic glycoantigens, together with the iNKT agonist α-GalCer, effectively enhances humoral immunity against carbohydrates and promotes class-switched IgG responses, thereby providing a basis for exploring glycan-targeting concepts in anti-helminth vaccine design.

Materials and Methods

Materials and General Methods

Unless otherwise noted, all chemicals and reagents were obtained from commercial suppliers and were used without further purification. General chemicals used for the synthesis were purchased from Acros, Merck Millipore, or Sigma-Aldrich. DOPC was purchased from Avanti Polar Lipids (Danvers, MA, USA). CH, EDC, palmitic acid, and DIPEA were obtained from an Exploration Platform (Shanghai, China). α-GalCer was purchased from Aladdin (USA). UDP-GalNAc and GDP-Fuc were obtained from Glycohub Pharmaceuticals (Wuhan, China). Galβ1-4(Fucα1-3)GlcNAc-βAsnFmoc (Le^x) and $GlcNAc_2Man_3GlcNAc_2$-βAsnFmoc (G0) were obtained from our laboratory. Thin-layer chromatography (TLC) was performed on Merck silica gel plates 60 F_{254}. Visualization was achieved under UV light (254 or 365 nm) or by treatment with 5% H_2SO_4/EtOH followed by heating. Reversed-phase chromatography medium (SP-120-50-ODS-RPS) was purchased from Daiso. Horseradish peroxidase (HRP)-conjugated goat anti-mouse IgG H&L was purchased from Abclonal (Wuhan, China), HRP-conjugated goat anti-mouse IgM from FineTest (Wuhan, China), HRP-conjugated Rabbit Anti-Mouse IgG1 mAb from Abclonal (Wuhan, China), HRP-conjugated Rabbit Anti-Mouse IgG2b (Fc) mAb from Abclonal (Wuhan, China), HRP-conjugated Goat Anti-Mouse IgG3 and HRP-conjugated goat anti-mouse IgG2c from SouthernBiotech (USA). TMB substrate was obtained from Beyotime Biotech (Shanghai, China). The cytokine kits for IFN-γ, IL-4, and IL-10 were provided by Eliret Biotechnology Company (Wuhan, China). PMA/Ionomycin mixture was provided by Lekong Biotechnology Company (Hangzhou, China). LPS was provided by Merck Company (Germany). Previously collected serum from *Schistosoma japonicum*-infected C57BL/6 mice and adult worm samples were obtained from our laboratory.

Dynamic light scattering (DLS) measurements were performed using a Zetasizer Nano ZS (ZEN3700, Malvern Instruments Ltd., Malvern, UK). Electron microscopy was performed using a transmission electron microscope (TEM) H-7650, Hitachi (Tokyo, Japan). ELISA data were obtained using Nunc MaxiSorp 96-well plates (Thermo Fisher Scientific, MA, USA) and read on a Spark microplate reader (Tecan, Switzerland). Nuclear magnetic resonance (NMR) spectra were recorded using a Bruker Ultrashield Plus 400 MHz spectrometer, Bruker Avance III 600 MHz spectrometer, or Bruker Advance III 800 MHz spectrometer with a TCI CryoProbe. ^1H and ^{13}C NMR spectra were referenced as follows: D_2O, δ 4.79 ppm for ^1H; CD_3OD, δ 3.31 ppm for ^1H and 49.00 ppm for ^{13}C; DMSO-d^6, δ 2.50 ppm for ^1H and 39.52 ppm for ^{13}C. High-resolution mass spectroscopy was performed using an ultra-high-performance liquid chromatography-high-resolution mass spectrometry system (Vanquish Q Exactive Plus, Thermo Fisher Scientific, USA).

Expression of CeGalNAcT and SmFucT-E in Insect Cells

The recombinant *Caenorhabditis elegans* β1,4-N-acetylgalactosaminyltransferase (*Ce*GalNAcT) and *S. mansoni* α1,3-fucosyltransferase-E (*Sm*FucT-E) used in this study were expressed and purified according to the following methods (Figure S1).[35,36] Briefly, the truncated genes encoding GalNAcT and FucT-E were individually cloned into the pFastBac baculovirus transfer vector and subsequently transformed into DH10Bac E. coli competent cells. Positive clones were selected via blue-white screening and white colonies were picked, cultured overnight, and used for recombinant bacmid DNA extraction. Purified bacmid DNA was then transfected into insect cells using the Lipofectamine™ transfection reagent (Beyotime) to generate the primary viral stock. After incubation at 28°C for 96 h, the culture supernatant containing the recombinant baculovirus was collected and used for a secondary large-scale infection of fresh insect cells to amplify protein production. After another 96 h of culture at 28°C, the supernatant containing secreted recombinant GalNAcT and FucT-E proteins was harvested. Target proteins were purified by nickel affinity chromatography and subsequently analyzed by SDS-PAGE (unpublished data).

Synthesis of LDN-βGlyFmoc (4) and LDNF-βGlyFmoc (5)

LDN-βGlyFmoc (**4**) and LDNF-βGlyFmoc (**5**) were synthesized via a chemo-enzymatic route using the chemically synthesized GlcNAcβGlyFmoc (**3**, Scheme S1) as the substrate. The synthesis proceeded through the successive enzymatic addition of an *N*-acetylgalactosamine residue followed by a fucose residue under optimized conditions.

Preparation of **4**: A standard reaction mixture (total volume: 5 mL) containing 4 mM substrate **3**, 6 mM UDP-GalNAc (1.5 equiv), 10 mM $MnCl_2$, 200 μg/mL *Ce*GalNAcT, and 100 mM Tris-HCl buffer (pH 8.0) was incubated at 37°C for 2 h. With the reaction completion confirmed by TLC (EtOAc/*i*-PrOH/H_2O, 4:2:1, v/v/v), the mixture was concentrated to remove the buffer. The crude product was purified using silica gel chromatography (eluent: CH_2Cl_2/MeOH, from 8:1 to 4:1) to afford **4** (12.2 mg, 87%) as a white solid. ^{1}H NMR (600 MHz, DMSO-d^6/D_2O 6:1): δ 7.85 (d, J = 7.5 Hz, 2H), 7.70–7.64 (m, 2H), 7.40 (t, J = 7.4 Hz, 2H), 7.32 (t, J = 7.4 Hz, 2H), 4.75 (d, J = 9.6 Hz, 1H), 4.33–4.20 (m, 4H), 3.75 (t, J = 9.5 Hz, 1H), 3.63–3.38 (m, 11H), 3.30–3.19 (m, 2H), 1.82, 1.80 (2s, 6H, 2NHAc). ^{13}C NMR (150 MHz, DMSO-d^6/D_2O 6:1): δ 171.89, 171.15, 170.87, 157.32, 144.49, 144.22, 141.30, 141.26, 128.45, 128.43, 127.88, 125.89, 125.79, 120.76, 102.87, 81.45, 79.47, 76.89, 76.16, 72.75, 71.38, 70.32, 67.90, 66.52, 63.32, 61.12, 60.10, 53.98, 52.54, 47.14, 43.90, 23.41, 23.10. HRMS (ESI) m/z calcd for **4** $[M+H]^+$ 703.2821 found 703.2820.

Preparation of **5**: A standard reaction mixture (total volume: 2.5 mL) containing 4 mM substrate **4**, 6 mM GDP-Fuc (1.5 equiv), 10 mM $MnCl_2$, 500 μg/mL *Sm*FucT-E, and 100 mM Tris-HCl buffer (pH 8.0) was incubated at 37°C for 48 h. The completion of the reaction was confirmed by TLC (EtOAc/*i*-PrOH/H_2O, 4:2:1, v/v/v) and the mixture was concentrated to remove the buffer. The crude product was purified by silica gel chromatography (eluent: CH_2Cl_2/MeOH, from 8:1 to 3:1) to afford **5** (6.4 mg, 76%) as a white solid. ^{1}H NMR (600 MHz, CD_3OD): δ 7.80 (d, J = 7.6 Hz, 2H), 7.68 (t, J = 8.1 Hz, 2H), 7.39 (t, J = 7.4 Hz, 2H), 7.31 (t, J = 7.4 Hz, 2H), 5.07 (d, J = 3.6 Hz, 1H), 5.00 (d, J = 9.3 Hz, 1H), 4.76 (q, J = 6.4 Hz, 1H), 4.49 (d, J = 8.3 Hz, 1H), 4.40–4.32 (m, 2H), 4.25 (t, J = 7.0 Hz, 1H), 4.06 (t, J = 9.2Hz, 1H), 3.96 (t, J = 9.8Hz, 1H), 3.93–3.62 (m, 12H), 3.57 (dd, J = 10.6, 2.6 Hz, 1H), 3.45–3.38 (m, 2H), 1.98, 1.97 (2s, 6H, 2NHAc), 1.27 (d, J = 6.5 Hz, 1H). ^{13}C NMR (150 MHz, CD_3OD): δ 174.18, 174.02, 172.96, 159.04, 145.42, 145.23, 142.61, 142.57, 128.78, 128.16, 126.31, 126.23, 120.92, 101.97, 100.06, 80.03, 79.17, 76.83, 76.42, 74.31, 73.79, 72.95, 71.56, 71.21, 69.91, 69.27, 68.22, 67.97, 62.83, 61.60, 55.44, 54.30, 48.32, 44.93, 23.02, 22.95, 16.73. HRMS (ESI) m/z calcd for **5** $[M+H]^+$ 849.3400 found 849.3398.

Synthesis of LDN-C16 (1) and LDNF-C16 (2)

Preparation of **1**: A mixture of **4** (5 mg, 7.0 μmol) and DMF/piperidine (9:1, v/v, 0.5 mL) was stirred at rt for 1 h. TLC (EtOAc/*i*-PrOH/H_2O, 4:2:1, v/v/v) showed that the reaction was complete. After the solvent was removed under reduced pressure, palmitic acid (2.7 mg, 10.5 μmol), *N*-ethyldiisopropylamine (DIPEA, 1.2 μL, 7.0 μmol), and ethyl dimethylaminopropyl carbodiimide (EDC, 2.2 mg, 14.2 μmol) was stirred in anhydrous DMF (0.2 mL) at room temperature under a nitrogen atmosphere for 12 h. TLC (EtOAc/*i*-PrOH/H_2O, 4:2:1, v/v/v) revealed that the reaction was complete. The solvent was removed and the crude product was purified using a reversed-phase column (eluent: 60% MeOH) to yield **1** (4.6 mg, 90%) as a white solid. ^{1}H NMR (600 MHz, DMSO-d^6/D_2O 6:1): δ 4.71 (d, J = 9.5 Hz, 1H), 4.29 (d, J = 8.5 Hz, 1H), 3.75 (t, J = 9.8 Hz, 1H), 3.65–3.38 (m, 11H), 3.26 (t, J = 8.3 Hz, 1H), 3.22–3.18 (m, 1H), 2.18–2.08 (m, 2H), 1.82, 1.79 (2s, 6H, 2NHAc), 1.49–1.40 (m, 2H), 1.25–1.15 (m, 24H), 0.81 (t, J = 6.7Hz, 3H). HRMS (ESI) m/z calcd for **1** $[M+H]^+$ 719.4437, found 719.4424.

Preparation of **2**: Compound **2** was prepared from compound **5** (5 mg, 5.9 μmol) in a manner analogous to that described for **1**, employing the same deprotection, coupling (with palmitic acid, DIPEA, and EDC), and purification procedure, affording **2** (4.5 mg, 88%) as a white solid. ^{1}H NMR (600 MHz, DMSO-d^6/D_2O 6:1): δ 4.83 (d, J = 3.5 Hz, 1H), 4.80 (d, J = 8.4 Hz, 1H), 4.53–4.45 (m, 1H), 4.28 (d, J = 8.5 Hz, 1H), 3.78–3.70 (m, 2H), 3.66–3.38 (m, 13H), 3.26–3.20 (m, 2H), 2.15–2.05 (m, 2H), 1.81, 1.80 (2s, 6H, 2NHAc), 1.48–1.40 (m, 2H), 1.25–1.14 (m, 24H), 1.05 (d, J = 6.1 Hz, 3H), 0.81 (t, J = 6.5Hz, 1H). ^{13}C NMR (150 MHz, DMSO-d^6/D_2O 6:1): δ 174.12, 171.65, 171.15, 170.50, 100.74, 98.97, 78.33, 77.78, 75.21, 72.83, 72.25, 71.28, 69.83, 68.48, 67.32, 66.76, 63.30, 60.56, 60.12, 52.55, 42.33, 35.68, 31.83, 29.53, 29.51, 29.45, 29.33, 29.22, 19.17, 25.59, 23.46, 23.10, 22.66, 16.85, 14.56. HRMS (ESI) m/z calcd for **2** $[M+H]^+$ 865.5016 found 865.5006.

Liposome Preparation

Liposomes were prepared using DOPC and CH as the main lipid components, together with cetyl-modified glycan antigens, either the disaccharide LDN-C16 or the trisaccharide LDNF-C16. The immunostimulatory adjuvant α-GalCer was incorporated into the selected formulations. Five distinct liposome formulations were prepared at specified molar ratios: ELP (empty liposome, DOPC:CH = 10:5), LP-LDN (DOPC:CH:LDN-C16 = 10:5:1), LP-LDN/G (DOPC:CH:LDN-C16:α-GalCer = 40:20:4:1), LP-LDNF (DOPC:CH:LDNF-C16 = 10:5:1), and LP-LDNF/G (DOPC:CH:LDNF-C16:α-GalCer = 40:20:4:1).

During preparation, lipid components were thoroughly dissolved in chloroform/methanol (2:1, v/v) and stirred at room temperature for 1 h. The solvent was removed by rotary evaporation to obtain a uniform film, which was freeze-dried for 12 h. The resulting powder was hydrated using HEPES buffer (20 mM, pH 7.4) and sonicated at 4°C for 25 min (5 s on, 5 s off).[37,38]

Liposome Characterization

Particle size and zeta potential were assessed by DLS on a Zetasizer Nano ZS, with measurements conducted at 25°C and a detector angle of 90°.[39,40] For particle size analysis, a 10 μL aliquot of the liposome suspension (5 mg/mL) was diluted with 3 mL of HEPES buffer (20 mM, pH 7.4). Zeta potential was determined using liposomes dispersed in HEPES buffer (20 mM, pH 7.4) at a concentration of 0.1 mg/mL, which were introduced into a capillary cell installed in the instrument. All measurements were performed in triplicate to derive the average values. To examine the morphology of the liposomes, a small drop of liposome dispersion (0.1 mg/mL) was applied to a 100-mesh copper grid, and excess liquid was absorbed using filter paper. A drop of 2% phosphotungstic acid solution (pH 7.4) was then applied to the grid, which was subsequently dried in a desiccator for 12 hours. The samples were imaged using TEM (H-7650).

Animal Immunization

Fifty-four female C57BL/6 mice (5–6 weeks old) were purchased from Cavens Laboratory Animal Co., Ltd. (Changzhou, China) and divided into nine groups. The five groups received subcutaneous injections of one of the following liposomal formulations (100 μL per mouse, each containing 12 μg of antigen LDN-C16 or LDNF-C16): ELP, LP-LDN, LP-LDN/G, LP-LDNF, or LP-LDNF/G. For comparison, four separate groups were administered 12 μg of the corresponding free antigen (LDN-C16 or LDNF-C16 with or without α-GalCer). Baseline serum samples were collected on day 0. Immunizations were then administered subcutaneously on days 1, 7, 14, 28, and 35. Blood samples (approximately 100 μL per mouse) were obtained from the tail vein on days 13, 20, 34, and 42 and were subsequently stored at 4°C for 12 h.

Preparation of Glycoconjugates

Four Fmoc-labeled glycan-compounds **4, 5**, Galβ1-4(Fucα1-3)GlcNAc-βAsnFmoc (Le^x), and $GlcNAc_2Man_3$ $GlcNAc_2$-βAsnFmoc (G0, a typical bi-antennary complex-type N-glycan) were dissolved in DMF containing 10% piperidine and stirred at room temperature for 1 h to remove the Fmoc group. After removing the solvent via rotary evaporation and lyophilization, each product was dissolved in 0.50 mL of a 4:1 mixture of DMF and 0.1 M phosphate buffer (pH 8.0). A 15-fold molar excess of the bifunctional crosslinker disuccinimidyl glutarate (DSG) was added and the reaction mixture was stirred gently at room temperature for 3–6 h. Unreacted DSG was removed by washing the mixture thrice with ethyl acetate. The activated sugar derivative was then resuspended in 0.1 M phosphate-buffered saline (PBS). BSA was added at a molar ratio of 1:30 (BSA to glycans) and the conjugation reaction was allowed to proceed under gentle stirring at room temperature for 2.5–3.0 days.[41,42] Glycoconjugates were purified and desalted by ultrafiltration centrifugation and glycoprotein concentrations were determined using a BCA assay kit.[43] The prepared glycoconjugates were lyophilized and stored at −20°C for subsequent ELISA experiments.

Determination of Cytokines Secreted by Ex Vivo Splenocytes

Spleens were aseptically harvested from naïve female C57BL/6 mice aged 6–8 weeks (n = 3 biological replicates) immediately after euthanasia via cervical dislocation. Single-cell suspensions were generated via mechanical dissociation of splenic tissue, followed by filtration through a sterile cell filter. Red blood cells were lysed with red blood cell lysis solution, and the spleen cells were suspended in RPMI 1640 medium supplemented with 10% fetal bovine serum (FBS), penicillin (100 U/mL), streptomycin (100 μg/mL), and 0.4 mM β-mercaptoethanol. Cell viability was assessed by trypan blue exclusion, and the viable cell concentration was adjusted to 1×10^6 cells/mL. The cells were seeded into 24-well plates (1 mL per well) and cultured for 24 h (4 h for IL-4 detection) at 37 °C in a humidified atmosphere containing 5% CO_2, either in medium alone (negative control) or in medium supplemented with the following stimuli: PMA/ionomycin mixture (1× working concentration, diluted from a 250× stock solution), LPS (1 μg/mL), BSA (50 μg/mL), LDN-BSA (50 μg/mL), and LDNF-BSA (50 μg/mL). Following incubation, culture supernatants were collected. The concentrations of target cytokines (IFN-γ, IL-4 and IL-10) in the supernatants were measured using commercial ELISA kits according to the manufacturer's instructions.

ELISA Analysis for Antibody Responses

Four distinct glycan-BSA conjugates were each dissolved in 0.10 M sodium bicarbonate buffer (pH 9.6) to prepare individual coating solutions at a concentration of 0.2 μg/mL. For the assay, 100 μL of the coating solution was added to each well of a 96-well plate and incubated at 37°C for 1 h. After removing the solution, the wells were washed thrice with PBST. Blocking was performed by adding 200 μL of 1% bovine serum albumin (BSA) in PBS per well and incubating at room temperature for 1 h, followed by three additional washes with PBST.

Individual or pooled mouse sera were serially diluted 3-fold in PBS (pH 7.4), from a 1:1500 dilution to 1:121,500. A volume of 100 μL of each diluted serum sample were added to each well and incubated at 37°C for 2 h. After washing thrice with PBST, 100 μL of HRP-conjugated goat anti-mouse secondary antibody (specific for Ig(G+M), IgG, or IgM; diluted 1:4000) was added to each well and incubated at room temperature for 1 h Following three final PBST washes, 100 μL of TMB substrate was added, and the plates were incubated in the dark at 25°C for 30 min. The absorbance was measured at 370 nm (OD_{370}) using a microplate reader.

Determination of Serum Cytokine Levels

Serum samples were collected from mice in each group and pooled. The concentrations of target cytokines (IFN-γ, IL-4, and IL-10) in the pooled sera were measured using commercial ELISA kits strictly according to the manufacturer's instructions. All assays were performed in triplicate to ensure reproducibility.

Preparation of Adult Worm Protein Extracts

Adult schistosome wormswere placed in RIPA lysis buffer supplemented with protease inhibitors and lysed by sonication on ice. The lysates were centrifuged at 12,000 × g for 15 min at 4°C. The resulting supernatant was collected and stored at –80°C for subsequent use.[44]

Western Blotting

Equal amounts of worm protein extracts were heated at 95°C for 10 min in loading buffer, separated on 10% SDS-PAGE gels at 90 V for 20 min followed by 180 V for 1 h, and then transferred onto PVDF membranes at 400 mA for 30 min on ice. Membranes were blocked with 5% non-fat milk in TBST for 1 h at room temperature. Subsequently, membranes were incubated for 1 h at RT with sera collected from different groups of mice (diluted 1:500 in TBST). After washing three times with TBST, membranes were incubated with HRP-conjugated goat anti-mouse IgG (1:5000) for 1 h at room temperature. Following three additional washes, immunoreactive bands were visualized using enhanced chemiluminescence (ECL) substrate.

Statistical Analysis

The ELISA was performed with pooled sera across three independent replicates, whereas assays involving individual sera were conducted as single measurements. The figure annotations provide the corresponding sample size (n), mean, and standard deviation (SD) for each dataset. All statistical analyses were conducted using GraphPad Prism software (version 10.1.2, California, USA). For comparisons between multiple groups at a single time point, one-way analysis of variance (ANOVA) was performed, followed by Dunnett's post-hoc test. For comparisons across multiple time points, two-way ANOVA with Tukey's multiple comparisons test was used. The cytokine detection was subjected to one-way analysis of variance (ANOVA), followed by Dunnett's post-hoc test. Statistical significance was set at $p < 0.05$.

Results

Synthesis of LDN-C16 and LDNF-C16

To enhance the immunogenicity of helminth glycans, cetyl (C16)-modified derivatives of the antigenic disaccharide (LDN-C16, **1**) and trisaccharide (LDNF-C16, **2**) were first synthesized and then assembled with DOPC, CH, and other components to form nanoliposomes.

The synthetic routes to compounds **1** and **2** are shown in Figure 2. The synthesis commenced with the chemically synthesized GlcNAcβGlyFmoc (**3**). Compound **3** was incubated with glycosyltransferase *Ce*GalNAcT and the glycosyl donor UDP-GalNAc in Tris-HCl buffer at 37°C for 2 h, affording the disaccharide derivative LDN-βGlyFmoc (**4**). TLC analysis indicated a near-quantitative conversion (data not shown). Subsequent purification by silica gel column chromatography afforded **4** in 87% yield. Next, fucosylation of **4** was carried out by incubation with glycosyltransferase *Sm*FucT-E and GDP-Fuc in Tris-HCl buffer at 37°C for 48 h, producing the trisaccharide LDNF-βGlyFmoc (**5**). Similarly, TLC monitoring confirmed an almost complete conversion (data not shown). Purification via silica gel column chromatography afforded compound **5** in a 76% yield. Compound **3** was prepared via amination of *N*-acetylglucosamine (**S1**) at the C-1 position, followed by coupling with Fmoc-Gly-Opfp (see Supporting Information for details).

To synthesize the lipid-modified derivative **1**, compound **4** was treated with 90% DMF/10% piperidine for 1 h to remove the Fmoc group. After lyophilization, the residue was coupled with palmitic acid in DMF overnight, using EDC and DIPEA as coupling agents. TLC chromatography confirmed the completion of the reaction. Product **1** was purified using reverse-phase column chromatography at an isolated yield of 90%. Following an analogous deprotection and coupling procedure, compound **5** was converted into the target glycolipid **2** with an isolated yield of 88%.

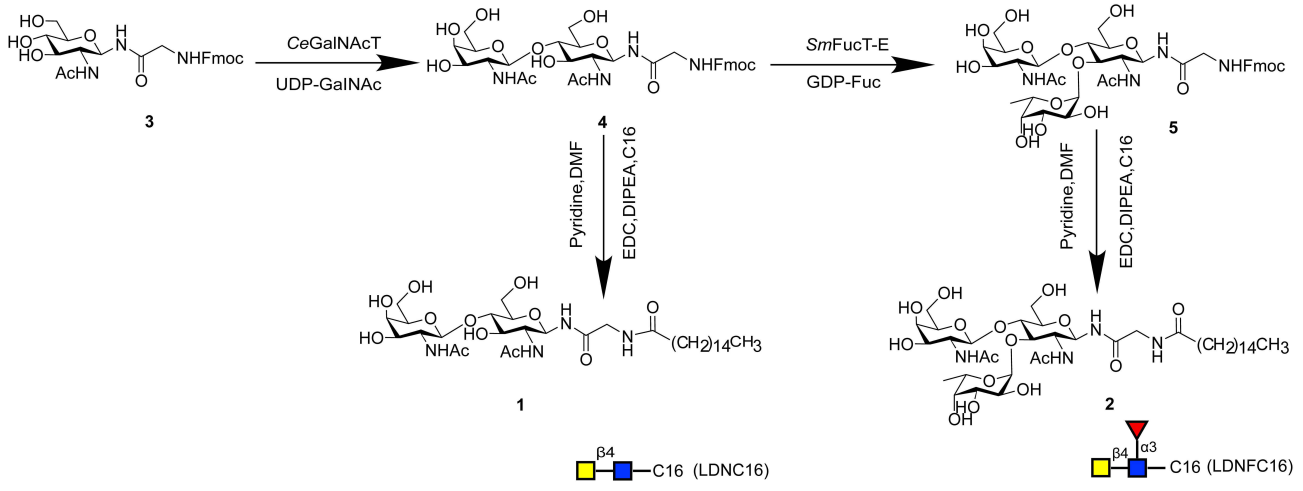

Figure 2 Chemo-enzymatic synthesis of LDN-C16 (**1**) and LDNF-C16 (**2**). The synthetic route began with GlcNAc-βGlyFmoc (**3**) as the substrate. LDN-βGlyFmoc (**4**, LacdiNAc intermediate) was synthesized from **3** by *Ce*GalNAcT with UDP-GalNAc as the sugar donor. *Sm*FucT-E then catalyzed the α1,3-fucosylation of **4** with GDP-Fuc to yield LDNF-βGlyFmoc (**5**, fucosylated LacdiNAc intermediate). Amide coupling of **4** and **5** with palmitic acid (mediated by EDC/DIPEA in pyridine/DMF) afforded the final products **1** and **2**, respectively.

Cytokine Responses to Glycan Stimulation in Splenocytes

To assess whether the helminth-derived glycans LDN and LDNF possess intrinsic immunostimulatory activity, we measured the IFN-γ, IL-4, and IL-10 levels in culture supernatants from naïve murine splenocytes after stimulation with glycan-BSA conjugates. As shown in Figure S2, splenocytes treated with BSA alone, LDN-BSA, or LDNF-BSA showed cytokine levels comparable to those detected in the unstimulated control (CK) group, with no significant increase observed for any of the three measured cytokines. In contrast, the positive control groups elicited robust, stimulus-specific responses: PMA/ionomycin stimulation induced marked IFN-γ production, accompanied by moderate upregulation of IL-4 and IL-10,[45] while LPS stimulation led to a pronounced increase in IL-10 levels.[46] These findings indicate that the LDN and LDNF glycan epitopes, in the absence of a delivery system or adjuvant, lack the intrinsic capacity to directly trigger cytokine responses in unprimed immune cells. This underscores the need to use a suitable delivery platform, such as liposomes, to enhance their immunogenicity in vivo.

Preparation and Characterization of Liposomes

Five distinct liposome formulations were prepared (Figure 3): **ELP** (empty liposome), **LP-LDN** (LDN-C16-loaded liposomes), **LP-LDN/G** (LDN-C16- and α-GalCer-loaded liposomes), **LP-LDNF** (LDNF-C16-loaded liposomes) and **LP-LDNF/G** (LDNF-C16 and α-GalCer-loaded liposomes). All formulations were prepared by the thin-film hydration method followed by sonication to reduce particle size and polydispersity. The composition of each liposome is shown in Table 1. Because particle size governs liposome biodistribution, stability, and antigen presentation,[47] we employed DLS to measure hydrodynamic diameter, PDI, and zeta potential and TEM to assess morphology.

As shown in Figure 4A, the size distribution profiles of all formulations were monomodal, indicating a homogeneous dispersion. The mean diameter of the empty ELP was 80.58 ± 3.22 nm. Incorporation of the antigenic glycolipids LDN-C16 and LDNF-C16 increased the mean diameters to 104.9 ± 0.52 nm (for LP-LDN) and 119.3 ± 4.64 nm (for LP-LDNF), respectively. Subsequent co-incorporation of α-GalCer further increased the sizes to 154.1 ± 3.42 nm (LP-LDN /G) and 155.9 ± 3.96 nm (LP-LDNF/G). PDI reflects the size distribution in a dispersion, ranging from 0 to 1.0, with PDI values >0.6, indicate a broad size distribution or the presence of large droplets and aggregates.[48] As summarized in Table 1, all antigen-loaded formulations exhibited markedly lower PDI values than the empty liposomes (PDI = 0.378), with values below 0.3, indicating narrow size distributions and favorable colloidal stability. Zeta potential (ζ) reflects the surface charge, which is critical for liposome stability and encapsulation efficiency. As the zeta potential increased in

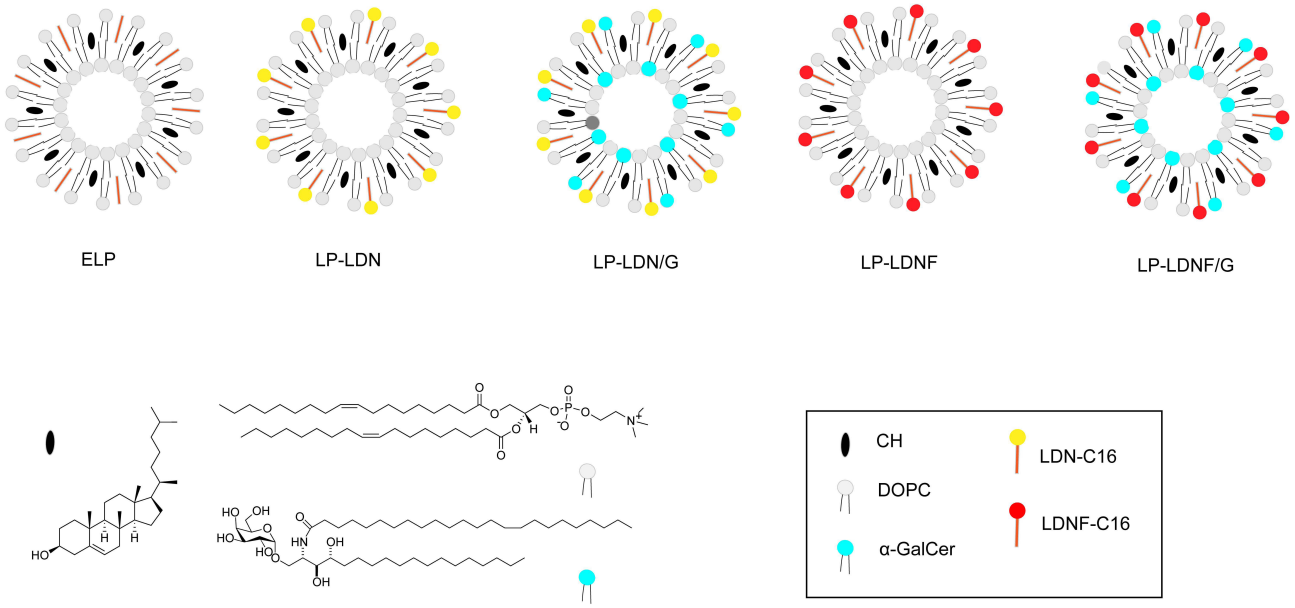

Figure 3 Schematic illustration of liposome formulations. The main chemical structures of five liposome compositions are depicted.

https://doi.org/10.2147/IJN.S590048

Table 1 Composition and Characterization of Liposome Formulations

Number	Composition (Molar Ratio)	Size (nm)	PDI	Zeta (mV)
I	DOPC:CH:C16 =10:5:2	80.58±3.22	0.378±0.366	−30.3±0.616
II	DOPC:CH:LDN-C16 =10:5:1	104.9±0.52	0.152±0.018	−11.8±0.499
III	DOPC:CH:LDN-C16:α-GalCer =40:20:4:1	154.1±3.42	0.102±0.011	−11.2±0.638
IV	DOPC:CH:LDNF-C16 =10:5:1	119.3±4.64	0.185±0.014	−19.3±1.027
V	DOPC:CH:LDNF-C16:α-GalCer =40:20:4:1	155.9±3.96	0.077±0.019	−17.2±0.613

magnitude, the electrostatic repulsion between the particles was enhanced, yielding a more stable colloidal dispersion.[49] As shown in Figure 4B, each zeta potential distribution curve exhibited a single peak, indicating a relatively uniformly dispersed state without obvious multiple populations or large aggregates. ELP, which contains palmitic acid (C16), exhibited a strongly negative surface charge (ζa≈ − 30 mV) at pH 7.4, owing to the deprotonated carboxylate groups.[50–52] Incorporation of neutral lipid-linked glycans (LDN-C16 or LDNF-C16) significantly attenuated the absolute zeta potential (–12 to –19 mV). This reduction confirms the successful glycolipid integration, which is attributable to the neutralization of the surface charge via amide bond formation and the shielding effect of the hydrated glycan headgroups.[53,54] The branched structure of LDNF leads to a slightly different packing of the headgroup and counterion distribution, resulting in a modestly more negative ζ than that of LDN.[55] The neutral α-GalCer has only a minimal additional impact on the surface charge.[56] Morphological analysis by TEM (Figure 4C) revealed that all five liposome formulations were spherical, well-dispersed, and intact, with sizes corroborating DLS measurements.

Mouse Immunization and Antibody Responses Analysis

To evaluate the effects of the newly formulated liposomal particles, immunization studies were conducted using C57BL/6 mice (five females per group). As illustrated in Figure 5A, mice were immunized subcutaneously on days 1, 7, 14, 28, and 35 to ensure sufficient immune stimulation.

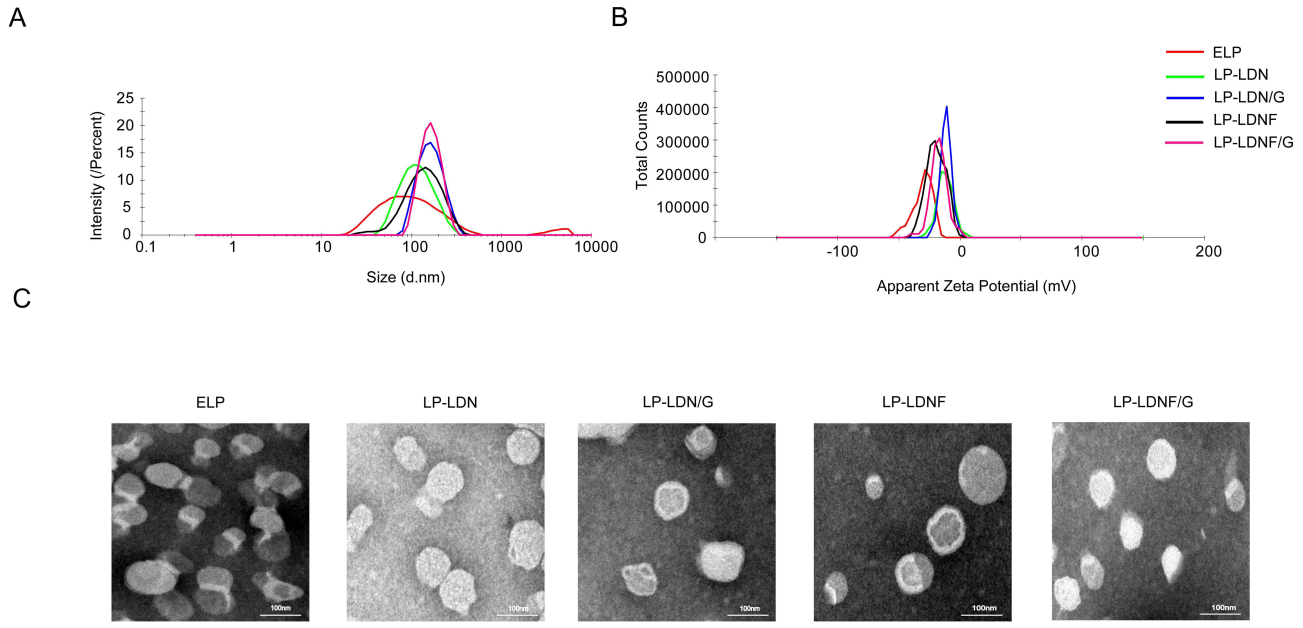

Figure 4 Characterization of liposomal formulations. (**A**) Particle size distribution profiles. (**B**) Zeta-potential distribution curves. (**C**) Representative transmission electron microscopy (TEM) images. Scale bar: 100 nm.

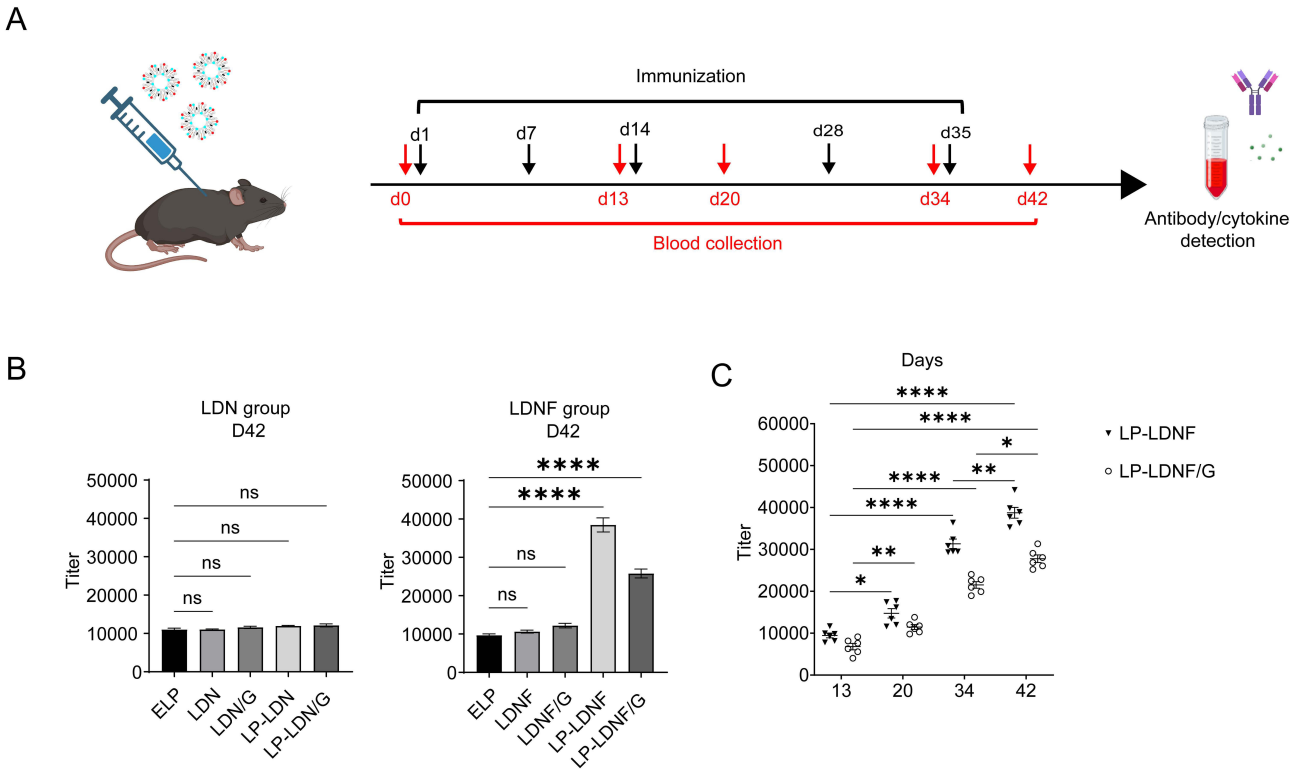

Figure 5 Evaluation of immunization efficacy and antibody dynamics in mice. (**A**) Schematic of the vaccination schedule. Female C57BL/6 mice received subcutaneous immunizations on days 1, 7, 14, 28, and 35. Sera were collected at Days 0, 13, 20, 34 and 42. Black arrows indicate immunization time points; red arrows indicate blood collection time points. (**B**) Total antibody (IgG+IgM) levels measured in sera at day 42. (**C**) Antibody titers elicited by LP-LDNF and LP-LDNF/G. LDN-BSA and LDNF-BSA were used as the coating antigen, respectively. Each line represents the average of sera from Days 13, 20, 34 and 42 from 5 replicate mice (each dot) and goat anti-mouse Ig (G+M). Statistical analysis was performed using one-way ANOVA with Dunnett's multiple comparisons test for comparisons within the same time point, and two-way ANOVA with Tukey's multiple comparisons test for comparisons across time points. (ns, $p > 0.05$; *$p < 0.05$; **$p < 0.01$; ****$p < 0.0001$).

Five liposomal formulations or control solutions containing free lipid-linked glycans with or without α-GalCer were injected into each group of mice. Serum samples were collected from individual mice on days 0 (baseline, prior to the first immunization), 13, 20, 34, and 42. Antisera were prepared and stored under standard conditions for subsequent antibody titer analysis.

Total antibody titers (IgG+IgM) against the LDN/LDNF antigen were determined by ELISA using sera collected on day 42 (Figure 5B). For LDN, all immunogen formulations, whether free or liposomal, induced titers that were statistically indistinguishable from that of the control (ELP), demonstrating minimal immunogenic potential. However, for LDNF, a clear divergence was observed: the free antigen was ineffective, whereas liposome-encapsulated LDNF-C16 (both LP-LDNF and LP-LDNF/G) was immunogenic, generating significantly elevated titers. The response to the α-GalCer-containing formulation (LP-LDNF/G) was slightly reduced relative to that of its adjuvant-free counterpart (LP-LDNF). This demonstrates that the immunogenicity of LDNF-C16 is contingent upon liposomal delivery, and the inclusion of α-GalCer may partially attenuate the response, possibly owing to changes in the physicochemical or pharmacokinetic properties of the carrier. Next, the two most immunogenic formulations, LP-LDNF and LP-LDNF/G, were selected for the longitudinal analysis of antibody kinetics (Figure 5C). Both groups exhibited a steady increase in total antibody titers following each booster immunization. The highest titers were observed one week after the fifth immunization (day 42), underscoring the necessity of repeated boosts to achieve and maintain peak humoral responses.

Analysis of Antibody Isotypes and IgG Subclasses

As both the LP-LDNF and LP-LDNF/G groups showed a sustained increase in antibody titers during booster immunizations, serum samples from day 42 were selected for antibody isotype analysis. As shown in Figure 6A, the LP-LDNF/G

https://doi.org/10.2147/IJN.S590048

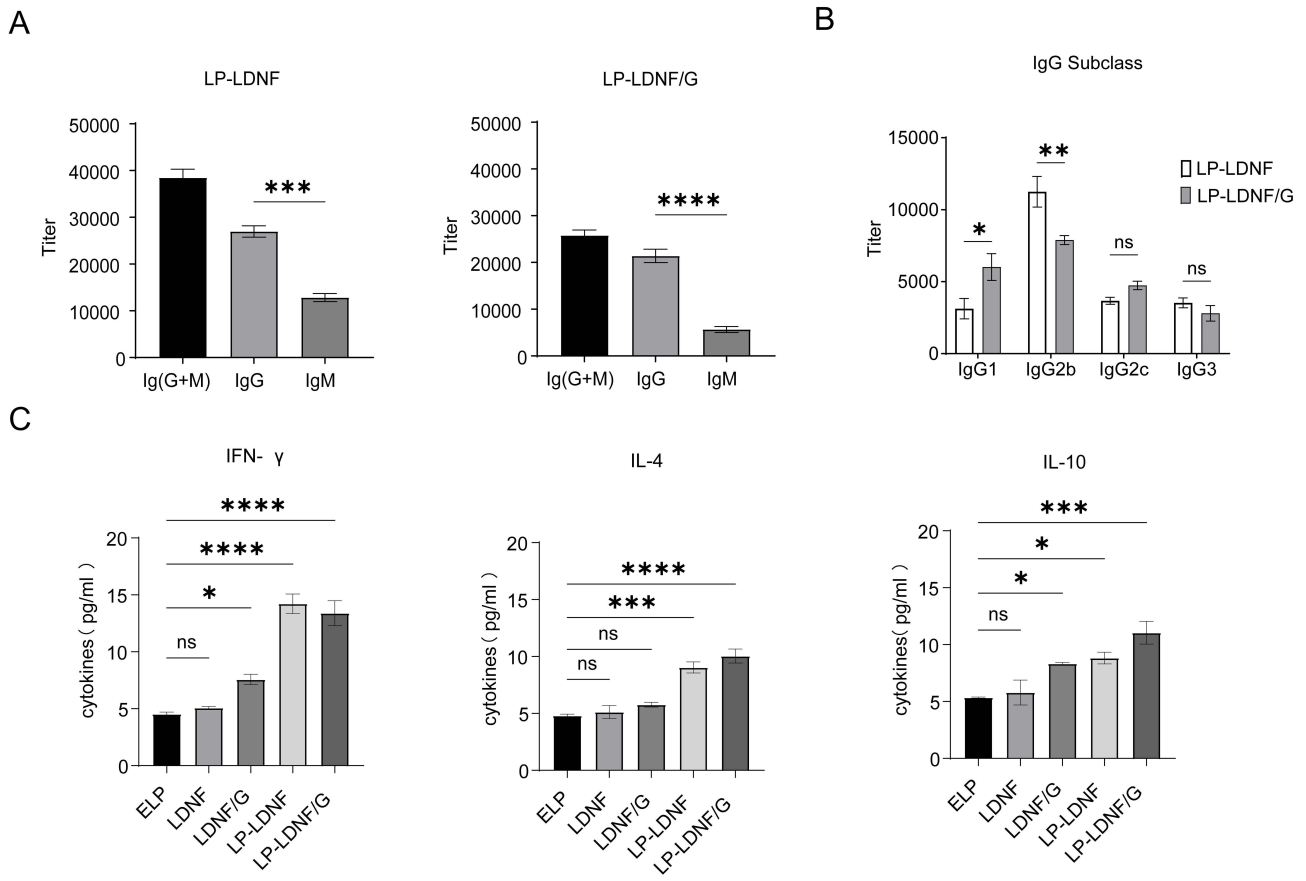

Figure 6 Profiling of antibody isotypes, IgG subclasses, and antigen specificity. (**A**) Antibody isotype analysis. Pooled sera from day 42 (LP-LDNF and LP-LDNF/G groups) were assessed using LDNF-BSA as the coating antigen. Total Ig(G+M), IgG, and IgM levels were detected with corresponding goat anti-mouse secondary antibodies. (**B**) IgG subclass profiling. Pooled sera from day 42 (LP-LDNF and LP-LDNF/G groups) were analyzed for IgG subclass distribution with LDNF-BSA as the coating antigen. (**C**) In vivo cytokine analysis. Pooled sera from day 42 (LDNF groups) were analyzed for IFN-γ, IL-4, IL-10. Statistical analysis was performed using one-way ANOVA with Dunnett's multiple comparisons test. (ns, *p < 0.05; **p < 0.01; ***p < 0.001; ****p < 0.0001).

group (with α-GalCer) exhibited a further increase in the ratio of IgG to IgM titers compared to the LP-LDNF group. This shift likely reflects α-GalCer-promoted B cell class switching and antibody maturation.[57]

We further compared the IgG subclass titers induced by the LP-LDNF and LP-LDNF/G groups (Figure 6B). Specifically, α-GalCer adjuvanticity manifested as a selective increase in IgG1 and decrease in IgG2b titers, with no significant change in IgG2c or IgG3. This indicates that α-GalCer reshapes the humoral response by qualitatively skewing the IgG isotype profile rather than uniformly enhancing all antibody subclasses.[58]

Serum Cytokine Responses to Different LDNF Formulations

To further characterize the immune responses elicited by different formulations of the LDNF glycan, we measured serum levels of IFN-γ, IL-4, and IL-10 in immunized mice at day 42 post-immunization (Figure 6C). The cytokine profiles varied markedly depending on the formulation, with a clear trend of increasing responses from free glycan to liposomal formulations.

Mice immunized with free LDNF-C16 exhibited cytokine levels comparable to those of the control (ELP) group, with all three cytokines remaining near baseline, indicating that the free glycan alone had limited capacity to induce systemic cytokine responses in vivo. Incorporation of α-GalCer into the free glycan formulation elicited a modest increase in cytokine levels.[59] In contrast, liposomal formulations of LDNF-C16 induced substantially stronger cytokine responses. Both LP-LDNF and LP-LDNF/G groups displayed significantly higher levels of all three cytokines compared to the free glycan groups, demonstrating that liposomal delivery markedly enhances the in vivo immunostimulatory activity of the LDNF glycan.[60] Comparison between the two liposomal groups revealed distinct cytokine profiles: LP-LDNF alone

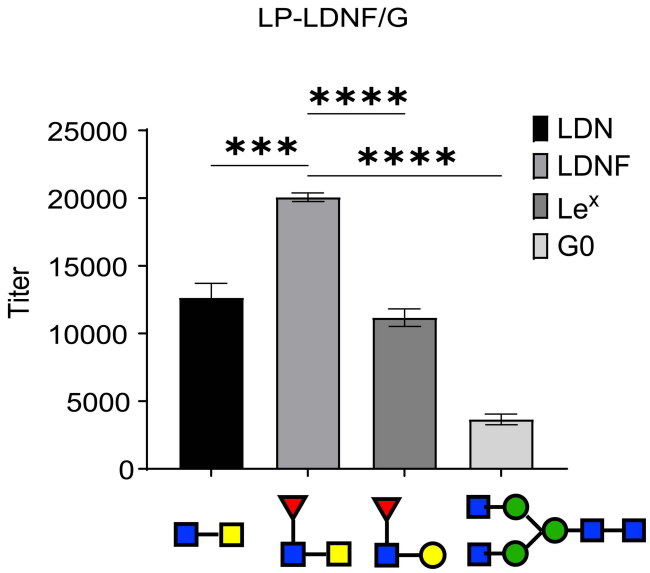

Figure 7 Antigen specificity of serum antibodies. Pooled sera from theday 42 LP-LDNF/G group were tested against apanel of glycoconjugates (LDN-BSA, LDNF-BSA, Le^x-BSA, and G0-BSA). Data points represent the mean of triplicate measurements. Statistical significance was determined by ordinary one-way ANOVA followed by Dunnett's multiple comparisons test (***$p < 0.001$; ****$p < 0.0001$).

induced the highest levels of IFN-γ, while incorporation of α-GalCer in LP-LDNF/G maintained elevated IFN-γ and further enhanced the production of IL-4 and IL-10. These results suggest that liposomal delivery of LDNF promotes robust cytokine responses, and the inclusion of α-GalCer modulates the cytokine microenvironment by augmenting Th2-type (IL-4) and regulatory (IL-10) cytokines while preserving a strong Th1-type (IFN-γ) response.

Specificity of IgG Antibodies Induced by LP-LDNF/G

The specificity of the IgG antibodies elicited by LP-LDNF/G was assessed using ELISA (Figure 7). The binding affinities of antisera to LDNF were compared with those of LDN, Le^x, and G0. The results demonstrated that IgG antibodies exhibited significantly higher affinity for the LDNF oligosaccharide than for the other glycans tested. These findings indicated that LP-LDNF can effectively stimulate the production of antigen-specific IgG antibodies.

Recognition of Schistosome Worm Proteins by Immune Serum

To evaluate the ability of antibodies induced by each immunization regimen to recognize native proteins from *Schistosoma japonicum* adult worms, Western blotting was performed using worm protein extracts as the antigen source (Figure S3). Sera collected from mice in each group were used as primary antibodies. The negative control group (unimmunized) exhibited only weak background bands, whereas serum from infected C57BL/6 mice recognized multiple distinct bands. Compared to the negative control, sera from the LP-LDN and LP-LDN/G groups also displayed relatively weak bands. In contrast, the LP-LDNF and LP-LDNF/G groups exhibited intense bands, with overall signal slightly higher than that observed in the LDN-related groups. These findings are consistent with the antibody response intensities observed following immunization. Furthermore, the recognition pattern of immune sera against adult worm proteins corresponded to the positions of LDNF-expressing protein bands reported in the literature for *Schistosoma japonicum* adult worms.[61]

Discussion

During parasitic infections, carbohydrate (glycan) antigens, which are abundantly expressed on the parasite's surface and in excretory/secretory products, serve as key targets for inducing specific antibodies in the host.[62] These antibodies exert protective effects by recognizing surface glycans, inhibiting pathogen growth, and preventing egg deposition.[8,63]

https://doi.org/10.2147/IJN.S590048

However, the structural complexity and synthetic difficulty of carbohydrate antigens pose major challenges for the development of glycan-based vaccines.

LDN and LDNF are antigenic glycan structures abundantly expressed on the surface of parasitic helminths, such as *Trichinella spiralis, Fasciola hepatica, Dictyocaulus viviparus* and various schistosome species.[64–66] To explore their vaccine potential, we first employed a chemo-enzymatic approach to synthesize the LDN and LDNF glycans. Using an ex vivo splenocyte stimulation assay, we observed that neither LDN nor LDNF glycans, when presented as BSA conjugates, induced significant cytokine production. This finding confirmed that these glycans lack inherent pro-inflammatory activity and require appropriate delivery systems to elicit robust immune responses in vivo. This observation aligns with the well-established notion that free oligosaccharides typically induce only weak antibody responses dominated by IgM.[67] Therefore, we employed liposome nanoparticles as a delivery platform to present these glycan antigens. Subsequently, both glycans were modified with a hexadecyl group to yield the hydrophobic derivatives, LDN-C16 and LDNF-C16. These hydrophobic derivatives were incorporated into liposomes either alone or in combination with the invariant natural killer T-cell agonist α-GalCer as an adjuvant. Such multivalent displays are expected to effectively drive B-cell receptor (BCR) cross-linking, leading to robust B-cell activation, and laying a structural foundation for potent immunogenicity.[21]

Next, we characterized the physicochemical properties of the five prepared liposomes, such as particle size, PDI, and Zeta potential. DLS and TEM analyses revealed that all liposomes exhibited an ideal monodisperse spherical structure (PDI < 0.3) with a uniform particle size (80–156 nm), which is conducive to stable circulation in vivo and effective capture by the immune system.[68] Zeta potential analysis further revealed that the incorporation of neutral glycolipids (LDN-C16/LDNF-C16) significantly neutralized the surface negative charge of the empty liposomes (ELP, $\zeta \approx -30$ mV), resulting in a final potential of −12 to −19 mV. This phenomenon can be attributed to the charge-neutralizing effect of the amide-linked glycolipids and steric shielding effect of the hydrated glycan chains.[53,54] These optimized surface characteristics not only enhance the colloidal stability of liposomes but also likely promote their efficient retention in lymph nodes and uptake by antigen-presenting cells (APCs), thereby laying a physical foundation for the subsequent robust immune response.[69,70] Following the subcutaneous immunization of C57BL/6 mice and analysis of the humoral immune response, we found that liposome-delivered LDN-C16 failed to elicit a significant antibody response. In contrast, liposome-delivered LDNF-C16 (with or without α-GalCer) significantly increased total antibody (IgG+IgM) titers in the later stage of immunization (day 42). This result directly demonstrated that LDNF possesses stronger immunogenicity than LDN, which is consistent with the results of previous studies. Fucosylated LDN (such as LDNF) is a highly immunogenic glycan structure that is recognized by host antibodies during infection. In contrast, LDN epitopes exert a weaker stimulation of the immune system.[11] This disparity likely stems from the parasitic immune evasion strategies. Many parasites dynamically alter their surface glycan expression during infection.[66] For example, after invading the host, schistosomes downregulate the expression of highly antigenic fucosylated structures, such as LDNF, and switch to expressing LDN, which more closely resembles host glycans, such as LN. This "molecular mimicry" strategy helps parasites evade immune surveillance.[9] Consequently, the strong immunogenicity of LDNF observed in this study provides indirect support for the active suppression of parasite expression during natural infection to minimize the risk of recognition by the host immune system. As a classic iNKT cell agonist, α-GalCer can rapidly drive the class switching of antibodies by activating iNKT cells and inducing the coordinated secretion of Th1 and Th2 cytokines, such as IFN-γ and IL-4.[71,72] In this study, the IgG/IgM ratio in the LP-LDNF/G group (containing α-GalCer) was statistically higher than that in the LP-LDNF group, confirming that α-GalCer effectively promoted class switching from IgM to IgG. Analysis of serum cytokine levels further supported this mechanism: compared to the LP-LDNF group, mice immunized with LP-LDNF/G exhibited elevated levels of both IFN-γ and IL-4, consistent with the known ability of α-GalCer to activate iNKT cells and promote Th1- and Th2-type cytokine production.[73] Further analysis of the IgG subclasses revealed that α-GalCer selectively upregulated IgG1 while decreasing IgG2b titers, while showing no significant effect on IgG2c and IgG3. This subclass profile aligns with the observed cytokine microenvironment, as the enhanced IL-4 production likely promoted switching to IgG1, whereas the concomitant increase in IL-10 may have contributed to the suppression of IgG2b responses.[73] Concurrently, repeated α-GalCer stimulation drives iNKT cells toward a low-responsiveness IL-10-producing NKT10 phenotype and expands IL-10-producing regulatory lymphocytes.[74] The elevated IL-10 levels detected in the LP-LDNF/G group are consistent with this reported phenomenon. IL-10 suppresses B-cell activation and alters class-switching pathways, particularly those leading to "intermediate" subclasses such as IgG2b.[75] These findings indicate that α-

GalCer reshapes the IgG subclass profile by modulating the cytokine environment and influencing B cell class-switching pathways.

The core of vaccine efficacy is the production of antibodies with protective function. In this study, ELISA confirmed that IgG antibodies induced by LP-LDNF/G exhibited high specific affinity for the LDNF epitope, with no significant cross-reactivity observed against structurally similar LDN, Le^x, or complex N-glycans (G0). This high specificity is a crucial characteristic of an ideal vaccine candidate as it minimizes off-target effects and potential autoimmune risks. This finding aligns with the larval-killing effect mediated by LDNF-specific IgG observed during natural infections,[76] strongly suggesting that the LDNF-C16 liposome vaccine constructed in this study can induce functionally relevant antibodies, showing promise in providing effective immune protection by blocking the invasion stage of the parasite.

In addition to evaluating glycan-specific humoral responses, we further assessed whether antibodies induced by the liposomal formulations could recognize native antigens expressed on *Schistosoma japonicum* adult worms. Western blot analysis revealed that sera from mice immunized with LP-LDNF and LP-LDNF/G recognized protein bands from worm extracts with intensities slightly higher than those observed in the LDN-immunized or control groups. This result demonstrates that antibodies elicited by the synthetic LDNF glycan are capable of binding to native parasite glycoproteins, likely through recognition of the same or structurally similar glycan epitopes presented in their natural context. The banding patterns observed were consistent with previously reported glycoproteins in *S. japonicum* known to carry LDNF motifs.[61] These findings support the translational potential of the liposomal LDNF platform, as the generated antibodies recognize not only synthetic glycan targets but also relevant parasite-derived antigens—a key prerequisite for functional anti-helminth immunity.

Our study demonstrated that liposomal co-delivery of LDNF and α-GalCer elicited strong immunogenicity and specific IgG responses. However, several key issues still require further refinement and validation in subsequent work. First, the antibody titers achieved could be further enhanced, which may be attributed to the limited immunostimulatory capacity of a single glycan epitope. Future strategies may include multivalent antigen design, such as co-presenting LDNF with other protective parasitic glycan epitopes to synergistically boost immune responses, as well as optimizing vaccine efficacy through adjustments in dosage, administration route, or combination with other adjuvants. Second, direct evidence for the hypothesized mechanism of action—whereby co-delivery facilitates APC uptake, leading to CD1d presentation, iNKT activation, and enhanced class switching—has not yet been established and warrants further in vitro investigation. These aspects are listed as priorities for future research to establish a more comprehensive chain of evidence. Finally, functional protection against live parasite challenge was not assessed in this study. Therefore, the current results primarily reflect evidence at the immunogenicity level and cannot be directly extrapolated to protective immunity. Although the induction of glycan-specific antibodies represents a crucial step toward protective immunity, direct evidence of vaccine efficacy in reducing parasite burden or preventing infection in vivo remains to be established. Future studies incorporating challenge models with relevant helminth species are essential to validate the translational potential of this liposome-based glycan vaccine.

Conclusion

In summary, we have developed a liposomal vaccine platform that co-delivers the synthetic helminth glycan LDNF together with the iNKT cell agonist α-GalCer. This strategy elicited robust, class-switched IgG responses with strong specificity for both synthetic and native parasite antigens, while also promoting a balanced cytokine profile. These findings validate the liposomal delivery approach for enhancing glycan immunogenicity. Future studies incorporating mechanistic dissection and parasite challenge models will be essential to translate these immunological insights into protective anti-helminth immunity.

Abbreviations

LN, Galβ1-4GlcNAc-R; LDN, GalNAcβ1-4GlcNAc-R; LDNF, GalNAcβ1-4(Fucα1-3)GlcNAc-R; ADCC, antibody-dependent cellular cytotoxicity; ES, excretory/secretory; α-GalCer, α-galactosylceramide; DOPC, dioleoylphosphatidylcholine; CH, cholesterol; DLS, Dynamic light scattering; TEM, transmission electron microscopy; NMR, Nuclear

magnetic resonance; DIPEA, *N*-ethyldiisopropylamine; EDC, Ethyldimethylaminopropyl Carbodiimide; DSG, disuccinimidyl glutarate; PBS, phosphate-buffered saline. LPS, Lipopolysaccharide.

Data Sharing Statement

All data generated or analyzed during this study are included in this published article and its Supplementary Information Files.

Ethics Approval and Consent to Participate

Animal experiments were conducted according to guidelines and protocols approved by the Ethics Committee of the Jiangsu Institute of Parasitic Diseases (approval number: JIPD-2024-009).

Consent for Publication

We confirm that all authors have read and agreed to the manuscript before submission.

Author Contributions

All authors made a significant contribution to the work reported, whether that is in the conception, study design, execution, acquisition of data, analysis and interpretation, or in all these areas; took part in drafting, revising or critically reviewing the article; gave final approval of the version to be published; have agreed on the journal to which the article has been submitted; and agree to be accountable for all aspects of the work.

Funding

This work was supported by a grant-in-aid from the Natural Science Foundation of China (No. 82373644), and the Natural Science Foundation of Jiangsu Province (No. BK20250299), and Scientific Research Project of the Health Commission of Jiangsu Province (No. M2025047), and Science and Technology Research Funds of the Wuxi TaihuLight Program (No. K20231043), and the Jiangsu Funding Program for Excellent Postdoctoral Talent to Qiang Chao.

Disclosure

The authors declare no conflict of interest.

References

1. Molla E, Mamo H. Soil-transmitted helminth infections, anemia and undernutrition among schoolchildren in Yirgacheffee, South Ethiopia. *BMC Res Notes*. 2018;11(1):585. doi:10.1186/s13104-018-3679-9
2. Badri M, Olfatifar M, Gharibi Z, et al. A systematic review and meta-analysis on the global prevalence of helminthic parasites among schoolchildren: a public health concern. *BMC Public Health*. 2025;25(1):2852. doi:10.1186/s12889-025-23958-9
3. Robinson MW, Sotillo J. Foodborne trematodes: old foes, new kids on the block and research perspectives for control and understanding host-parasite interactions. *Parasitology*. 2022;149(10):1257–1261. doi:10.1017/s0031182022000877
4. Thompson RCA. Zoonotic helminths - why the challenge remains. *J Helminthol*. 2023;97e21. doi:10.1017/s0022149x23000020
5. Chatterji T, Khanna N, Alghamdi S, et al. A recent advance in the diagnosis, treatment, and vaccine development for human schistosomiasis. *Trop Med Infect Dis*. 2024;9(10). doi:10.3390/tropicalmed9100243
6. Smit CH, van Diepen A, Nguyen DL, et al. Glycomic analysis of life stages of the human parasite *Schistosoma mansoni* reveals developmental expression profiles of functional and antigenic glycan motifs. *Mol Cell Proteomics*. 2015;14(7):1750–1769. doi:10.1074/mcp.M115.048280
7. Cummings RD. "Stuck on sugars - how carbohydrates regulate cell adhesion, recognition, and signaling". *Glycoconj J*. 2019;36(4):241–257. doi:10.1007/s10719-019-09876-0
8. Prasanphanich NS, Mickum ML, Heimburg-Molinaro J, Cummings RD. Glycoconjugates in host-helminth interactions. *Front Immunol*. 2013;4:240. doi:10.3389/fimmu.2013.00240
9. Van Die I, Cummings RD. Glycan gimmickry by parasitic helminths: a strategy for modulating the host immune response? *Glycobiology*. 2010;20(1):2–12. doi:10.1093/glycob/cwp140
10. Hokke CH, van Diepen A. Helminth glycomics – glycan repertoires and host-parasite interactions. *Mol Biochem Parasitol*. 2017;215:47–57. doi:10.1016/j.molbiopara.2016.12.001
11. Bunte MJM, Schots A, Kammenga JE, Wilbers RHP. Helminth glycans at the host-parasite interface and their potential for developing novel therapeutics. *Front Mol Biosci*. 2021;8:807821. doi:10.3389/fmolb.2021.807821
12. Hussaarts L, Yazdanbakhsh M, Guigas B. Priming dendritic cells for th2 polarization: lessons learned from helminths and implications for metabolic disorders. *Front Immunol*. 2014;5:499. doi:10.3389/fimmu.2014.00499

13. Naus CW, van Remoortere A, Ouma JH, et al. Specific antibody responses to three schistosome-related carbohydrate structures in recently exposed immigrants and established residents in an area of *Schistosoma mansoni* endemicity. *Infect Immun*. 2003;71(10):5676–5681. doi:10.1128/iai.71.10.5676-5681.2003
14. Petralia LMC, van Diepen A, Nguyen DL, et al. Unraveling cross-reactivity of anti-glycan IgG responses in filarial nematode infections. *Front Immunol*. 2023;14:1102344. doi:10.3389/fimmu.2023.1102344
15. Luyai AE, Heimburg-Molinaro J, Prasanphanich NS, et al. Differential expression of anti-glycan antibodies in schistosome-infected humans, rhesus monkeys and mice. *Glycobiology*. 2014;24(7):602–618. doi:10.1093/glycob/cwu029
16. Nyame AK, Lewis FA, Doughty BL, Correa-Oliveira R, Cummings RD. Immunity to schistosomiasis: glycans are potential antigenic targets for immune intervention. *Exp Parasitol*. 2003;104(1–2):1–13. doi:10.1016/s0014-4894(03)00110-3
17. Vervelde L, Bakker N, Kooyman FN, et al. Vaccination-induced protection of lambs against the parasitic nematode haemonchus contortus correlates with high IgG antibody responses to the LDNF glycan antigen. *Glycobiology*. 2003;13(11):795–804. doi:10.1093/glycob/cwg107
18. Khatun F, Toth I, Stephenson RJ. Immunology of carbohydrate-based vaccines. *Adv Drug Deliv Rev*. 2020;165-166:117–126. doi:10.1016/j.addr.2020.04.006
19. Kappler K, Hennet T. Emergence and significance of carbohydrate-specific antibodies. *Genes Immun*. 2020;21(4):224–239. doi:10.1038/s41435-020-0105-9
20. Zhao T, Cai Y, Jiang Y, et al. Vaccine adjuvants: mechanisms and platforms. *Signal Transduct Target Ther*. 2023;8(1):283. doi:10.1038/s41392-023-01557-7
21. Ols S, Lenart K, Arcoverde Cerveira R, et al. Multivalent antigen display on nanoparticle immunogens increases B cell clonotype diversity and neutralization breadth to pneumoviruses. *Immunity*. 2023;56(10):2425–2441.e14. doi:10.1016/j.immuni.2023.08.011
22. Archambault MJ, Tshibwabwa LM, Côté-Cyr M, Moffet S, Shiao TC, Bourgault S. Nanoparticles as delivery systems for antigenic saccharides: from conjugation chemistry to vaccine design. *Vaccines*. 2024;12(11). doi:10.3390/vaccines12111290
23. De Guinoa J S, Jimeno R, Gaya M, et al. CD1d-mediated lipid presentation by CD11c(+) cells regulates intestinal homeostasis. *EMBO j*. 2018;37(5). doi:10.15252/embj.201797537
24. Guo T, Chamoto K, Nakatsugawa M, et al. Mouse and human CD1d-Self-Lipid complexes are recognized differently by murine invariant natural killer T cell receptors. *PLoS One*. 2016;11(5):e0156114. doi:10.1371/journal.pone.0156114
25. Florence WC, Bhat RK, Joyce S. CD1d-restricted glycolipid antigens: presentation principles, recognition logic and functional consequences. *Expert Rev Mol Med*. 2008;10(e20). doi:10.1017/s1462399408000732
26. Moody DB, Besra GS, Wilson IA, Porcelli SA. The molecular basis of CD1-mediated presentation of lipid antigens. *Immunol Rev*. 1999;172:285–296. doi:10.1111/j.1600-065x.1999.tb01373.x
27. Diupotex M, Zamora-Chimal J, Cervantes-Sarabia RB, Salaiza-Suazo N, Becker I. Alpha-galactosylceramide as adjuvant induces protective cell-mediated immunity against Leishmania mexicana infection in vaccinated BALB/c mice. *Cell Immunol*. 2023;386:104692. doi:10.1016/j.cellimm.2023.104692
28. Subrahmanyam P, Webb TJ. Boosting the immune response: the use of iNKT cell ligands as vaccine adjuvants. *Front Biol*. 2012;7(5):436–444. doi:10.1007/s11515-012-1194-2
29. Wang P, Huo CX, Lang S, et al. Chemical synthesis and immunological evaluation of a pentasaccharide bearing multiple rare sugars as a potential anti-pertussis vaccine. *Angew Chem Int Ed Engl*. 2020;59(16):6451–6458. doi:10.1002/anie.201915913
30. Gao Y, Wang W, Yang Y, et al. Developing next-generation protein-based vaccines using high-affinity glycan ligand-decorated glyconanoparticles. *Adv Sci*. 2023;10(2):e2204598. doi:10.1002/advs.202204598
31. Zeissig S, Olszak T, Melum E, Blumberg RS. Analyzing antigen recognition by natural killer T cells. *Method Mol Biol*. 2013;960:557–572. doi:10.1007/978-1-62703-218-6_41
32. Yu KO, Im JS, Molano A, et al. Modulation of CD1d-restricted NKT cell responses by using N-acyl variants of alpha-galactosylceramides. *Proc Natl Acad Sci U S A*. 2005;102(9):3383–3388. doi:10.1073/pnas.0407488102
33. Schulte S, Sukhova GK, Libby P. Genetically programmed biases in Th1 and Th2 immune responses modulate atherogenesis. *Am J Pathol*. 2008;172(6):1500–1508. doi:10.2353/ajpath.2008.070776
34. Wakeham J, Wang J, Xing Z. Genetically determined disparate innate and adaptive cell-mediated immune responses to pulmonary mycobacterium bovis BCG infection in C57BL/6 and BALB/c mice. *Infect Immun*. 2000;68(12):6946–6953. doi:10.1128/iai.68.12.6946-6953.2000
35. Kawar ZS, Van Die I, Cummings RD. Molecular cloning and enzymatic characterization of a UDP-GalNAc:GlcNAc(beta)-R beta1,4-N-acetylgalactosaminyltransferase from *Caenorhabditis elegans*. *J Biol Chem*. 2002;277(38):34924–34932. doi:10.1074/jbc.M206112200
36. Van Noort K, Nguyen DL, Kriechbaumer V, et al. Functional characterization of *Schistosoma mansoni* fucosyltransferases in Nicotiana benthamiana plants. *Sci Rep*. 2020;10(1):18528. doi:10.1038/s41598-020-74485-z
37. Jia JX, Kalisa NY, Lu TT, Zhou Z, Gao XD, Wang N. Chemo-enzymatic synthesis of the ALG1-CDG biomarker and evaluation of its immunogenicity. *Bioorg Med Chem Lett*. 2020;30(24):127614. doi:10.1016/j.bmcl.2020.127614
38. Liao G, Zhou Z, Suryawanshi S, Mondal MA, Guo Z. Fully synthetic self-adjuvanting α-2,9-oligosialic acid based conjugate vaccines against group C meningitis. *ACS Cent Sci*. 2016;2(4):210–218. doi:10.1021/acscentsci.5b00364
39. Jia JX, Peng SL, Kalisa NY, et al. A liposomal carbohydrate vaccine, adjuvanted with an NKT cell agonist, induces rapid and enhanced immune responses and antibody class switching. *J Nanobiotechnology*. 2023;21(1):175. doi:10.1186/s12951-023-01927-x
40. Depalo N, Fanizza E, Vischio F, et al. Imaging modification of colon carcinoma cells exposed to lipid based nanovectors for drug delivery: a scanning electron microscopy investigation. *RSC Adv*. 2019;9(38):21810–21825. doi:10.1039/c9ra02381j
41. Zhang H, Wang X, Meng Y, Yang X, Zhao Q, Gao J. Total synthesis of the tetrasaccharide haptens of vibrio vulnificus MO6-24 and BO62316 and immunological evaluation of their protein conjugates. *JACS Au*. 2022;2(1):97–108. doi:10.1021/jacsau.1c00190
42. Mylvaganam M, Lingwood CA. A convenient oxidation of natural glycosphingolipids to their "Ceramide acids" for neoglycoconjugation: BOVINE SERUM ALBUMIN-GLYCOSYLCERAMIDE ACID CONJUGATES AS INVESTIGATIVE PROBES FOR HIV gp120 COAT PROTEIN-GLYCOSPHINGOLIPID INTERACTIONS*. *Journal of Biological Chemistry*. 1999;274(29):20725–20732. doi:10.1074/jbc.274.29.20725
43. Smith PK, Krohn RI, Hermanson GT, et al. Measurement of protein using bicinchoninic acid. *Analytical Biochemistry*. 1985;150(1):76–85. doi:10.1016/0003-2697(85)90442-7
44. Hunter KS, Davies SJ. Host adaptive immune status regulates expression of the schistosome AMP-Activated Protein Kinase. *Front Immunol*. 2018;9:2699. doi:10.3389/fimmu.2018.02699

45. Guo L, Urban JF, Zhu J, Paul WE. Elevating calcium in Th2 cells activates multiple pathways to induce IL-4 transcription and mRNA stabilization. *J Immunol*. 2008;181(6):3984–3993. doi:10.4049/jimmunol.181.6.3984
46. Xu H, Liew LN, Kuo IC, Huang CH, Goh DL, Chua KY. The modulatory effects of lipopolysaccharide-stimulated B cells on differential T-cell polarization. *Immunology*. 2008;125(2):218–228. doi:10.1111/j.1365-2567.2008.02832.x
47. Bachmann MF, Jennings GT. Vaccine delivery: a matter of size, geometry, kinetics and molecular patterns. *Nat Rev Immunol*. 2010;10 (11):787–796. doi:10.1038/nri2868
48. Danaei M, Dehghankhold M, Ataei S, et al. Impact of particle size and polydispersity index on the clinical applications of lipidic nanocarrier systems. *Pharmaceutics*. 2018;10(2). doi:10.3390/pharmaceutics10020057
49. Gopi S, Balakrishnan P. Evaluation and clinical comparison studies on liposomal and non-liposomal ascorbic acid (vitamin C) and their enhanced bioavailability. *J Liposome Res*. 2021;31(4):356–364. doi:10.1080/08982104.2020.1820521
50. Yanagihara S, Yuba E, Harada A. The impact of size for liposomes modified with pH-responsive β-glucan derivatives on the initiation of cellular and humoral immune responses in murine models. *Biotechnol Biotechnol Equip*. 2024;38(1):2358992. doi:10.1080/13102818.2024.2358992
51. Yanagihara S, Kitayama Y, Yuba E, Harada A. Preparing size-controlled liposomes modified with polysaccharide derivatives for ph-responsive drug delivery applications. *Life*. 2023;13(11). doi:10.3390/life13112158
52. Chibowski E, Szcześ A. Zeta potential and surface charge of DPPC and DOPC liposomes in the presence of PLC enzyme. *Adsorption*. 2016;22 (4):755–765. doi:10.1007/s10450-016-9767-z
53. Day AH, Adams SJ, Gines L, et al. Synthetic routes, characterization and photophysical properties of luminescent, surface functionalized nanodiamonds. *Carbon*. 2019;152:335–343.
54. Stefaniu C, Latza VM, Gutowski O, Fontaine P, Brezesinski G, Schneck E. Headgroup-Ordered monolayers of uncharged glycolipids exhibit selective interactions with ions. *J Phys Chem Lett*. 2019;10(8):1684–1690. doi:10.1021/acs.jpclett.8b03865
55. Mukhina T, Brezesinski G, Shen C, Schneck E. Phase behavior and miscibility in lipid monolayers containing glycolipids. *J Colloid Interface Sci*. 2022;615:786–796. doi:10.1016/j.jcis.2022.01.146
56. Guevara ML, Jilesen Z, Stojdl D, Persano S. Codelivery of mRNA with α-galactosylceramide using a new lipopolyplex formulation induces a strong antitumor response upon intravenous administration. *ACS Omega*. 2019;4(8):13015–13026. doi:10.1021/acsomega.9b00489
57. Lang Gillian A, Shrestha B, Amadou Amani S, Shadid Tyler M, Ballard Jimmy D, Lang Mark L. α-Galactosylceramide-reactive NKT cells increase IgG1 class switch against a clostridioides difficile polysaccharide antigen and enhance immunity against a live pathogen challenge. *Infect Immun*. 2021;89(11). doi:10.1128/iai.00438-21
58. Devera TS, Joshi SK, Aye LM, Lang GA, Ballard JD, Lang ML. Regulation of anthrax toxin-specific antibody titers by natural killer T cell-derived IL-4 and IFNγ. *PLoS One*. 2011;6(8):e23817. doi:10.1371/journal.pone.0023817
59. Fujii S, Shimizu K, Kronenberg M, Steinman RM. Prolonged IFN-gamma-producing NKT response induced with alpha-galactosylceramide-loaded DCs. *Nat Immunol*. 2002;3(9):867–874. doi:10.1038/ni827
60. Broecker F, Götze S, Hudon J, et al. Synthesis, liposomal formulation, and immunological evaluation of a minimalistic carbohydrate-α-galcer vaccine candidate. *J Med Chem*. 2018;61(11):4918–4927. doi:10.1021/acs.jmedchem.8b00312
61. Nyame AK, Leppänen AM, Bogitsh BJ, Cummings RD. Antibody responses to the fucosylated LacdiNAc glycan antigen in *Schistosoma mansoni*-infected mice and expression of the glycan among schistosomes. *Exp Parasitol*. 2000;96(4):202–212. doi:10.1006/expr.2000.4573
62. Prasanphanich NS, Luyai AE, Song X, et al. Immunization with recombinantly expressed glycan antigens from *Schistosoma mansoni* induces glycan-specific antibodies against the parasite. *Glycobiology*. 2014;24(7):619–637. doi:10.1093/glycob/cwu027
63. Van Diepen A, der Velden NS V, Smit CH, Meevissen MH, Hokke CH. Parasite glycans and antibody-mediated immune responses in Schistosoma infection. *Parasitology*. 2012;139(9):1219–1230. doi:10.1017/s0031182012000273
64. Mickum ML, Prasanphanich NS, Heimburg-Molinaro J, Leon KE, Cummings RD. Deciphering the glycogenome of schistosomes. *Front Genet*. 2014;5:262. doi:10.3389/fgene.2014.00262
65. Smit CH, Homann A, van Hensbergen VP, et al. Surface expression patterns of defined glycan antigens change during *Schistosoma mansoni* cercarial transformation and development of schistosomula. *Glycobiology*. 2015;25(12):1465–1479. doi:10.1093/glycob/cwv066
66. Verissimo CM, Graeff-Teixeira C, Jones MK, Morassutti AL. Glycans in the roles of parasitological diagnosis and host-parasite interplay. *Parasitology*. 2019;146(10):1217–1232. doi:10.1017/S0031182019000465
67. Velupillai P, Harn DA. Oligosaccharide-specific induction of interleukin 10 production by B220+ cells from schistosome-infected mice: a mechanism for regulation of CD4+ T-cell subsets. *Proc Natl Acad Sci U S A*. 1994;91(1):18–22. doi:10.1073/pnas.91.1.18
68. Jovanović AA, Petrović P, Pirković A, et al. Ergosterol-enriched liposomes with post-processing modifications for serpylli herba polyphenol delivery: physicochemical, stability and antioxidant assessment. *Pharmaceutics*. 2025;17(11). doi:10.3390/pharmaceutics17111362
69. Qin H, Teng Y, Dai R, Wang A, Liu J. Glycan-based scaffolds and nanoparticles as drug delivery system in cancer therapy. *Front Immunol*. 2024;15:1395187. doi:10.3389/fimmu.2024.1395187
70. Budhadev D, Poole E, Nehlmeier I, et al. Glycan-Gold nanoparticles as multifunctional probes for multivalent lectin-carbohydrate binding: implications for blocking virus infection and nanoparticle assembly. *J Am Chem Soc*. 2020;142(42):18022–18034. doi:10.1021/jacs.0c06793
71. Hayashizaki K, Kamii Y, Kinjo Y. Glycolipid antigen recognition by invariant natural killer T cells and its role in homeostasis and antimicrobial responses. *Front Immunol*. 2024;15:1402412. doi:10.3389/fimmu.2024.1402412
72. Vomhof-DeKrey EE, Yates J, Leadbetter EA. Invariant NKT cells provide innate and adaptive help for B cells. *Curr Opin Immunol*. 2014;28:12–17. doi:10.1016/j.coi.2014.01.007
73. Brailey PM, Lebrusant-Fernandez M, Barral P. NKT cells and the regulation of intestinal immunity: a two-way street. *Febs J*. 2020;287 (9):1686–1699. doi:10.1111/febs.15238
74. Sag D, Krause P, Hedrick CC, Kronenberg M, Wingender G. IL-10-producing NKT10 cells are a distinct regulatory invariant NKT cell subset. *J Clin Invest*. 2014;124(9):3725–3740. doi:10.1172/jci72308
75. Stanic B, van de Veen W, Wirz OF, et al. IL-10-overexpressing B cells regulate innate and adaptive immune responses. *J Allergy Clin Immunol*. 2015;135(3):771–80.e8. doi:10.1016/j.jaci.2014.07.041
76. Mickum ML, Prasanphanich NS, Song X, et al. Identification of antigenic glycans from *Schistosoma mansoni* by using a shotgun egg glycan microarray. *Infect Immun*. 2016;84(5):1371–1386. doi:10.1128/iai.01349-15